Crystal structures of hydroxylamine and a 15-crown-5 hydroxylaminosolvate: first observation of a cyclic hydroxylamine dimer $(NH_2OH)_2$

Mher A. Navasardyan, Danila R. Chernyavskiy and Mikhail V. Vener

N.S.Kurnakov Institute of General and Inorganic Chemistry, Russian Academy of Sciences, Leninskii prosp. 31, 119991 Moscow, Russia.

1. Experimental details. References.

1.1. Synthesis of neat hydroxylamine (I)

1.2. Synthesis of the 15-crown-5 hydroxylaminosolvate (II)

1.3. X-ray diffraction

2. Figures S1–S7

Fig. S1. Temperature dependence of the unit cell parameter *a* for a hydroxylamine NH_2OH single crystal (I).

Fig. S2. Temperature dependence of the unit cell parameter *b* for a hydroxylamine NH_2OH single crystal (I).

Fig. S3. Temperature dependence of the unit cell parameter *c* for a hydroxylamine NH_2OH single crystal (I).

Fig. S4. Temperature dependence of the unit cell volume V for the hydroxylamine NH_2OH molecular structure (I).

Fig. S5. Temperature dependence of the calculated density for a hydroxylamine NH_2OH single crystal (I).

Fig. S6. Decomposition of the 15-crown-5 hydroxylaminosolvate (II) in Fomblin® YR-1800 perfluorinated oil at –15 °C.

Fig. S7. Hydrogen-bonded chains in the structure REGRAW, SOWKEX (CCDC) and **II**.

Figures S8–S15. Deformation electron density maps for structures I (100–275 K) and II (100 K) obtained via NoSpherA2 refinements.

Tables S1-S5.

Table S1. Crystallographic data and selected parameters of X-ray structural analysis for the molecular structures of hydroxylamine at various temperatures (**I-100 – I-275**).

Table S2. Distances and angles describing hydrogen bonds in the structures of neat hydroxylamine at different temperatures (I-100 – I-275) and hydroxylaminosolvate 15-crown-5 (II).

Table S3. Crystallographic data and selected parameters of X-ray structural analysis for the molecular structure of the 15-crown-5 hydroxylaminosolvate (II).

Table S4. Intramolecular bond lengths (Å) and angles (°) in hydroxylamine: literature data from 1955 (*), neat hydroxylamine at various temperatures (I-100 – I-275), and the 15-crown-5 hydroxylaminosolvate (II).

Table S5. Crystalline structures containing hydroxylamine in zwitterionic ($NH_3^+O^-$) or neutral (NH_2OH) form.

Details of periodic (solid-state) DFT calculations. References.

Table S6. Distance between "heavy" atoms d(O···N)/d(N···O) of hydrogen bonds in the studied crystals. Experiment vs. periodic DFT computations in the and B3LYP/6-31G** and PBE-D3/6-31G** levels. Units are Å.

Table S7. The electron density ρ_b and its Laplacian $\nabla^2\rho_b$ at the (3,-1) critical point of intermolecular hydrogen bonds in crystals I and II calculated using periodic DFT computations in the and B3LYP/6-31G** and PBE-D3/6-31G** levels.

Selection criteria for statistical analysis

Table S8. Statistical parameters of N–O bond lengths for NH_2OH, $NH_3^+O^-$ and NH_3OH^+.

Fig. S16. Statistical analysis of N–O bond lengths and the 3σ criterion for NH_2OH, $NH_3^+O^-$ and NH_3OH^+.

1. Experimental details

1.1. Synthesis of neat hydroxylamine (I).

The synthesis was carried out following a modified procedure described by Hurd [s1-s2].

Solution 1: potassium *tert*-butoxide (3.15 g, 28.1 mmol) was dissolved in absolute butanol (20 mL).

Solution 2: finely ground hydroxylammonium chloride (2.5 g, 36.0 mmol) was dried on a rotary evaporator, suspended in absolute butanol (2.4 mL) and stirred for 20 min.

Solution 1 was added dropwise to solution 2 under vigorous stirring (1500 rpm) over 4.5 h, maintaining the pH at ca. 7.5. The precipitated KCl was filtered off on a Schott filter, washed with a small amount of absolute butanol, and then several times with absolute diethyl ether. The mother liquor was kept in a freezer at –35 °C for two weeks.

Large needle-shaped crystals of hydroxylamine (up to 1.5 cm in length) were obtained. These crystals were used for subsequent cocrystallisation.

1.2. Synthesis of the 15-crown-5 hydroxylaminosolvate (II).

Several crystals of hydroxylamine were placed in a 2 mL vial and kept at room temperature. The crystals melted, yielding approximately 0.4 mL of liquid hydroxylamine. 15-Crown-5 ether (0.2 mL) was added to the resulting liquid. The vial was placed in a freezer at –44 °C for 2 h, then removed and left at room temperature. After two days, colourless needle- and plate-shaped crystals were formed.

1.3. X-ray diffraction.

Caution: The crystals of both I and II were highly unstable in air when removed from the mother liquor and prone to rapid degradation at room temperature due to potential decomposition, melting, or extreme hygroscopicity. Therefore, they were rapidly selected from the solution and mounted at –15 °C under a protective layer of Fomblin® YR-1800 perfluorinated oil using a Linkam CMS196 cooling stage (controlled by a Linkam T96-P unit, Linkam Scientific Instruments Ltd, UK).

X-ray diffraction data for **I** (multi-temperature, 100–275 K) and **II** (100 K) were collected on a Bruker D8 Venture Photon diffractometer using graphite-monochromatized Mo-Kα radiation (λ = 0.71073 Å, Incoatec IμS 3.0 microfocus source) in φ and ω-scanning modes. Initial indexing, unit cell refinements, and reflection integrations were performed using the Bruker APEX3 package [s3]. Absorption corrections were applied using measured intensities of equivalent reflections [s4-

s5]. The structures were solved by direct methods and refined by the full-matrix least-squares method on F^2 anisotropically for all non-hydrogen atoms [s6-s7]. All hydrogen atoms were located from Fourier difference maps and refined isotropically.

In addition to the independent atom model (IAM) refinement described above, all structures of I (multi-temperature data sets) and II were re-refined using the NoSpherA2 approach [s8] implemented within Olex2 [s9] using the olex2.refine engine [s10] with non-spherical form factors (r2SCAN functional, cc-pVTZ basis set). The molecular wavefunctions were calculated iteratively using the ORCA (version 6.0) quantum chemistry package [s11]. In these refinements, all hydrogen atoms were refined with anisotropic displacement parameters, providing accurate, neutron-like hydrogen positions.

The obtained crystal data, including atomic coordinates, bond lengths, bond angles, and structure refinements of **I** (100-275 K) and **II** were deposited with the Cambridge Crystallographic Data Centre (CCDC numbers 2557401-2557416, respectively, https://www.ccdc.cam.ac.uk/structures/).

References

s1. C. D. Hurd, L. F. Audrieth and L. A. Nalefski, in *Inorganic Syntheses*, ed. H. S. Booth, Wiley, 1st edn., 1939, vol. 1, pp. 87–89.

s2. G. Albertin, S. Antoniutti, J. Bravo, J. Castro, S. García-Fontán, M. C. Marín and M. Noè, *Eur J Inorg Chem*, 2006, **2006**, 3451–3462.

s3. APEX3, SAINT and SADABS. Madison, Wisconsin, USA: Bruker AXS, **2016**.

s4. G.M. Sheldrick. SADABS: Program for Scaling and Correction of Area Detector Data. Gottingen, Germany: University of Gottingen, **1997**.

s5. SADABS, Ver. 2016/2: Area Detector Scaling and Absorption Correction Program. Karlsruhe, Germany: Bruker AXS, **2016**.

s6. G.M. Sheldrick. SHELXT – Integrated space-group and crystal-structure determination. *Acta Crystallogr*., *Sect*. *A: Found*. *Adv*., **2015**, *71*(1), 3–8. https://doi.org/10.1107/s2053273314026370

s7. G.M. Sheldrick. Crystal structure refinement with SHELXL. *Acta Crystallogr*., *Sect*. *C: Struct*. *Chem*., **2015**, *71*(1), 3–8. https://doi.org/10.1107/s2053229614024218

s8. F. Kleemiss, O. V. Dolomanov, M. Bodensteiner, N. Peyerimhoff, L. Midgley, L. J. Bourhis, A. Genoni, L. A. Malaspina, D. Jayatilaka, J. Lübben, H. Puschmann and S. Grabowsky, Accurate crystal structures and chemical properties from NoSpherA2, Chem. Sci., 2021, 12, 1675–1692. https://doi.org/10.1039/D0SC05526C

s9. O. V. Dolomanov, L. J. Bourhis, R. J. Gildea, J. A. K. Howard and H. Puschmann, OLEX2: a complete structure solution, refinement and analysis program, J. Appl. Crystallogr., 2009, 42, 339–341. https://doi.org/10.1107/S0021889808042726

s10. L. J. Bourhis, O. V. Dolomanov, R. J. Gildea, J. A. K. Howard and H. Puschmann, The anatomy of a comprehensive constrained, restrained refinement program for the modern computing environment – Olex2 dissected, Acta Cryst. A, 2015, 71, 59–75. https://doi.org/10.1107/S2053273314022207

s11. F. Neese, Software Update: The ORCA Program System—Version 6.0, WIREs Comput. Mol. Sci., 2025, 15(2), e70019. https://doi.org/10.1002/wcms.70019

2. Figures S1–S5

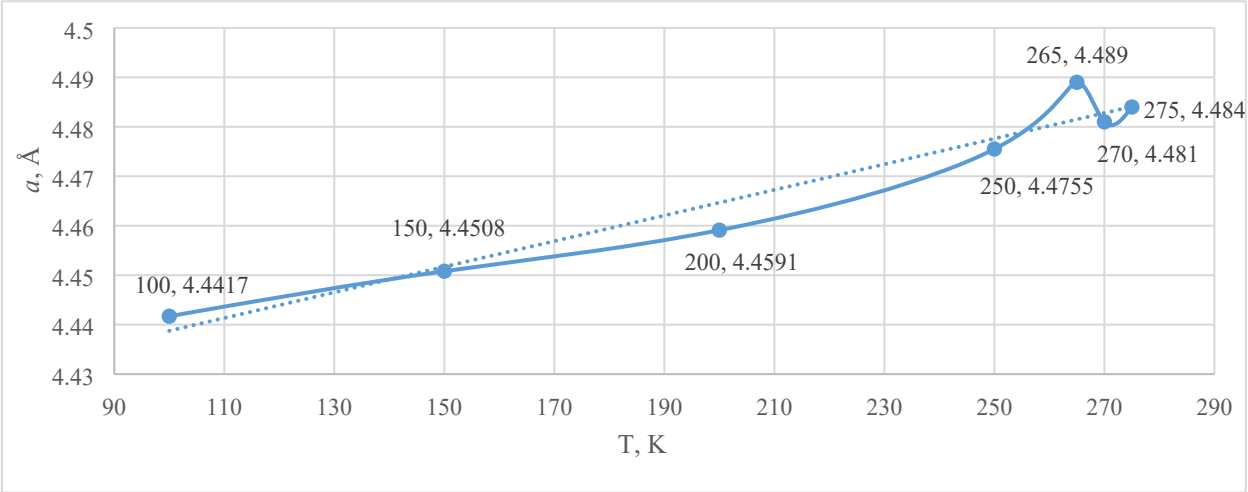

Fig. S1. Temperature dependence of the unit cell parameter *a* for a hydroxylamine NH_2OH single crystal (I).

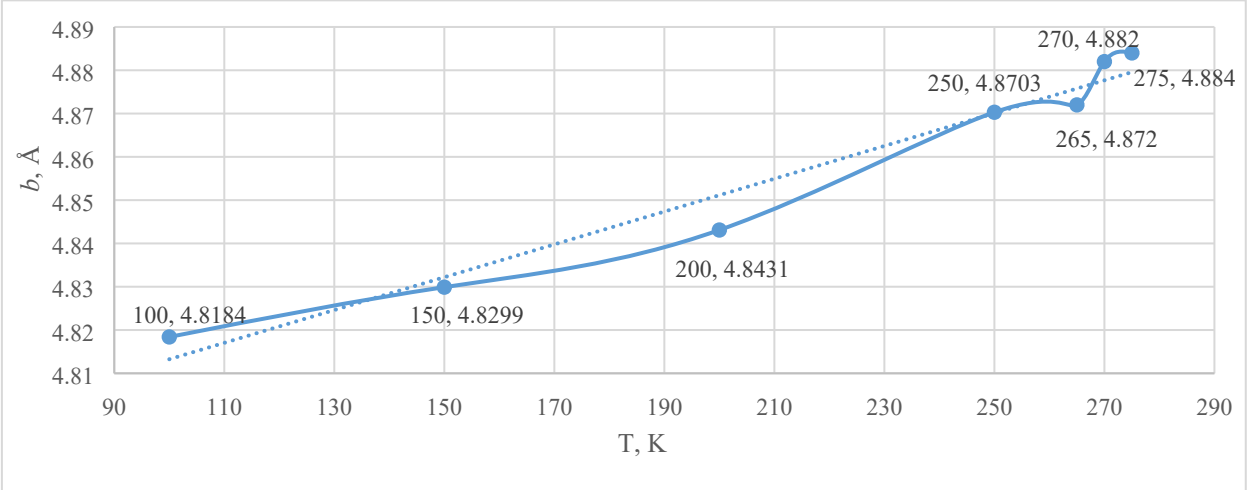

Fig. S2. Temperature dependence of the unit cell parameter *b* for a hydroxylamine NH_2OH single crystal (I).

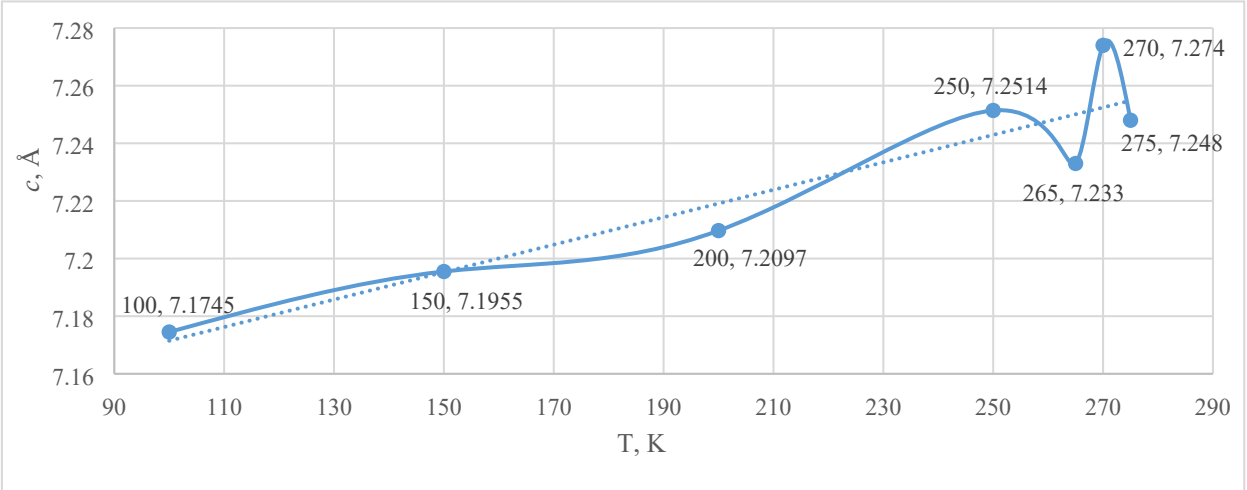

Fig. S3. Temperature dependence of the unit cell parameter *c* for a hydroxylamine NH_2OH single crystal (I).

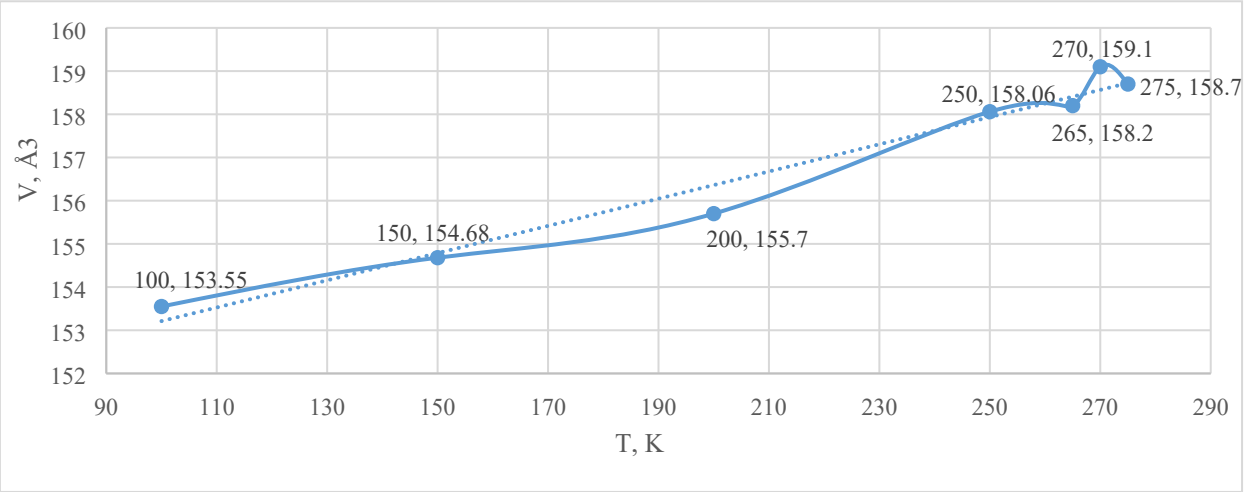

Fig. S4. Temperature dependence of the unit cell volume V for the hydroxylamine NH_2OH molecular structure (I).

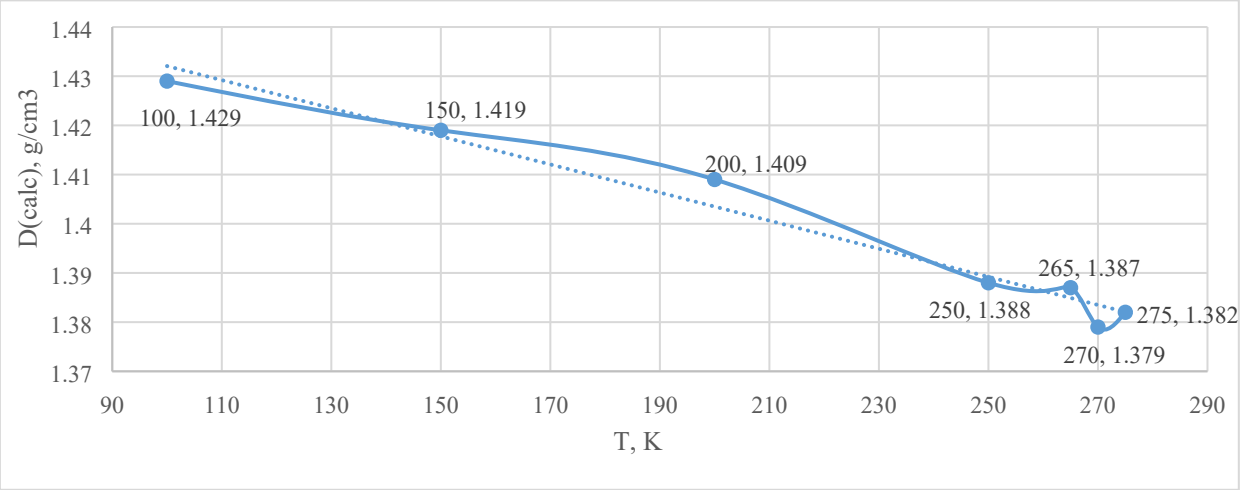

Fig. S5. Temperature dependence of the calculated density for a hydroxylamine NH_2OH single crystal (I).

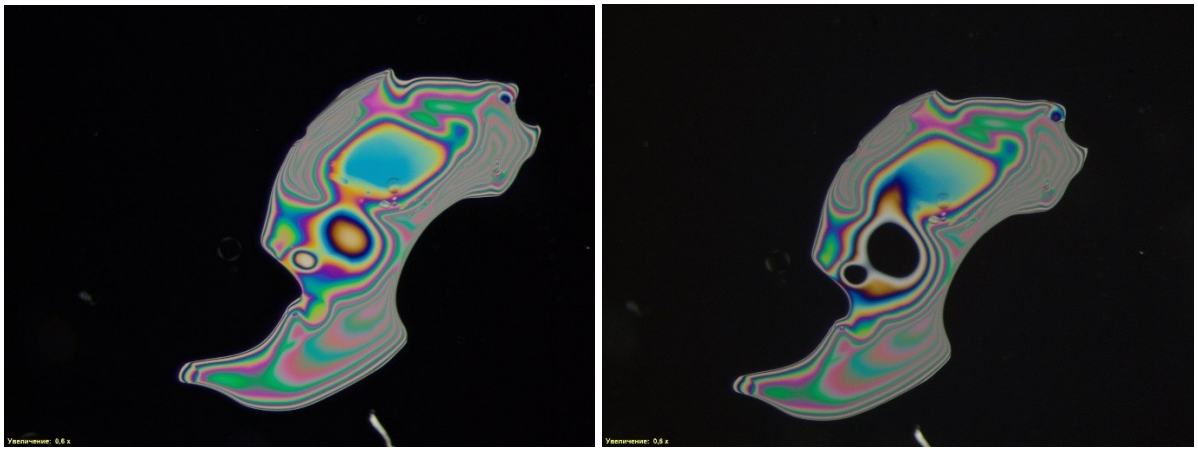

Fig. S6. Decomposition of the 15-crown-5 hydroxylaminosolvate (**II**) under a protective layer of Fomblin® YR-1800 perfluorinated oil, observed at –15 °C on a Linkam CMS196 cooling stage. It is worth noting that the crystal deteriorates from the center outward rather than from the edges. Images were captured using an Olympus SZ61 stereomicroscope.

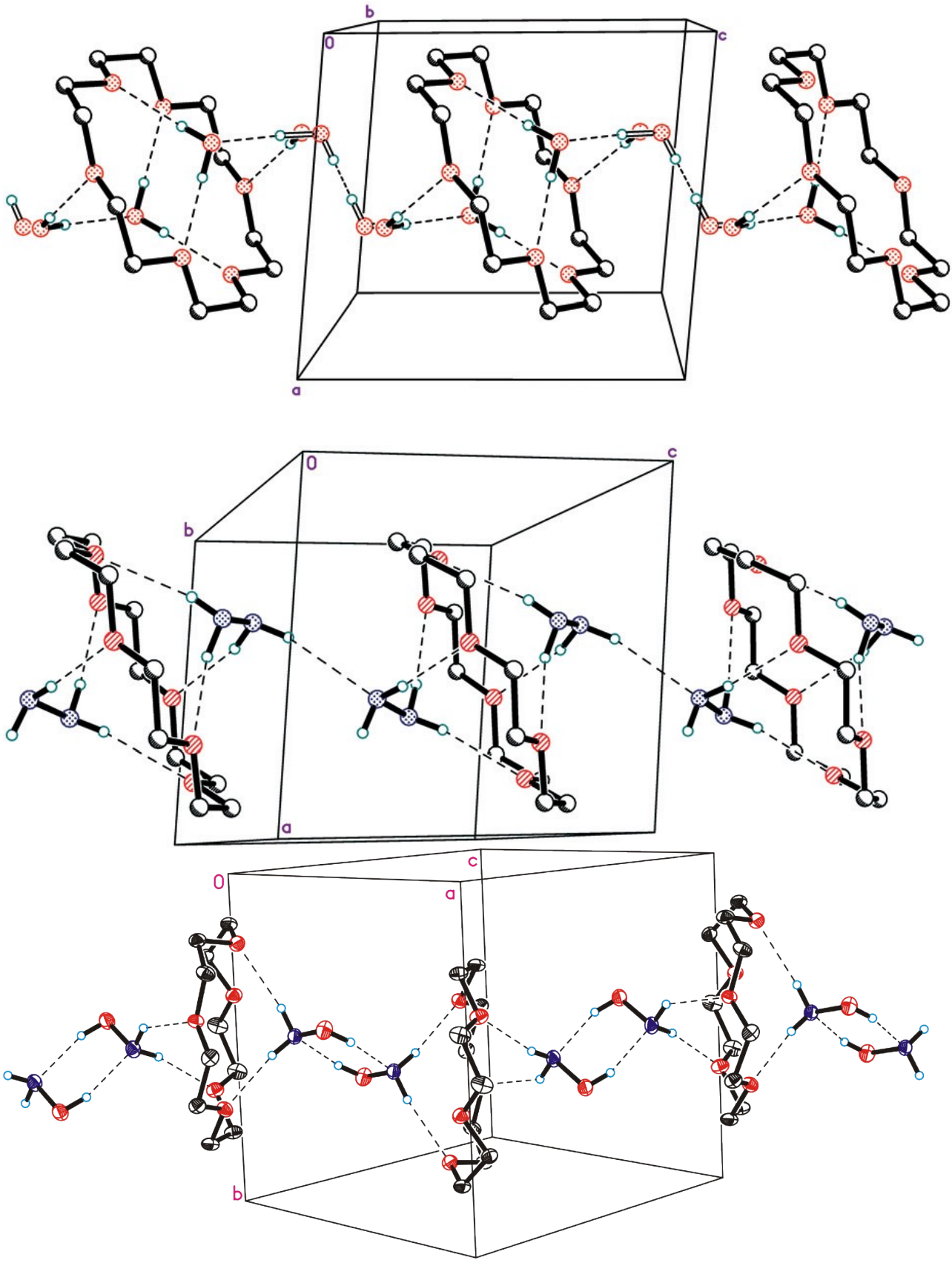

Fig. S7. Hydrogen-bonded chains in the structure REGRAW01, SOWKEX (CCDC) and **II**. Disordered water molecules are shown by open lines. Hydrogen bonds are drawn with dashed lines. 18-crown-6 hydrate and hydrazinosolvate; 15-crown-5 hydroxylaminosolvate.

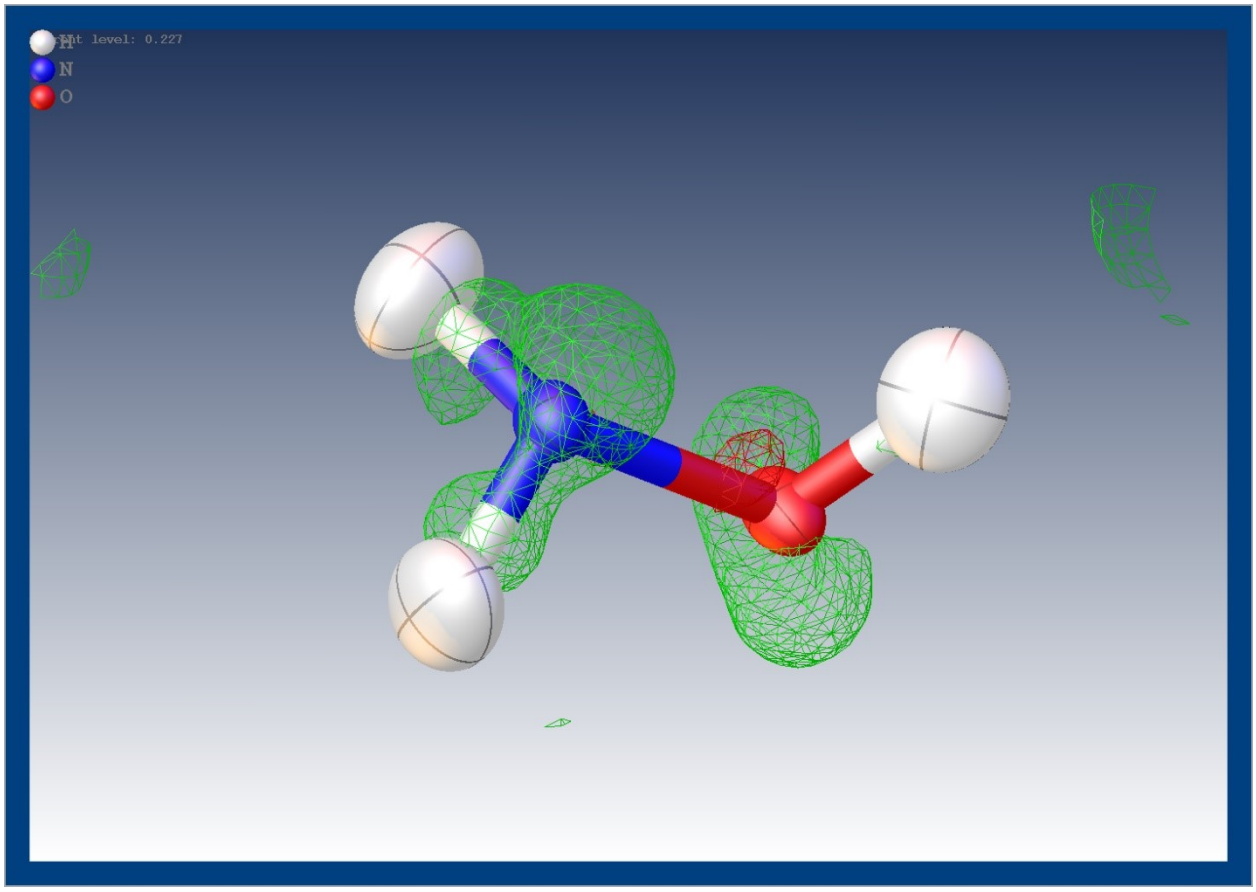

Fig. S8. Deformation electron density map of hydroxylamine (NH_2OH) crystal structure I-100 at 100 K. The green and red meshes represent positive and negative deformation densities, respectively, highlighting electron accumulation in chemical bonds and lone pairs, calculated with Olex2 using NoSpherA2 (r2SCAN/cc-pVTZ) wave-functions, plotted with an iso-value of 0.227 e/Å³. Anisotropic hydrogen atoms are represented at the 50% probability level.

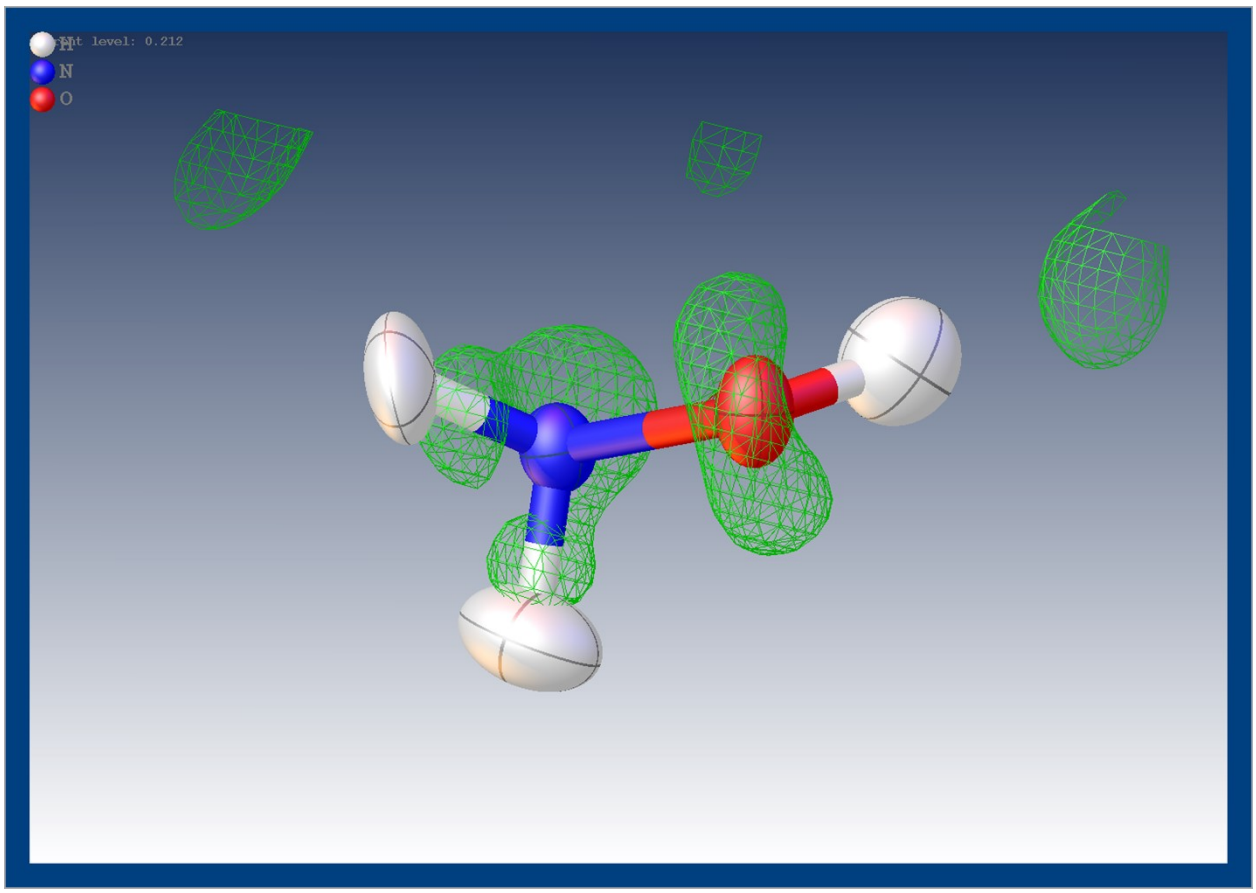

Fig. S9. Deformation electron density map of hydroxylamine (NH_2OH) crystal structure I-100 at 100 K. The green mesh represents positive deformation density, highlighting electron accumulation in chemical bonds and lone pairs (negative deformation density is not observed at this contour level). Calculated with Olex2 using NoSpherA2 (r2SCAN/cc-pVTZ) wave-functions, plotted with an iso-value of 0.212 e/Å^3. Anisotropic hydrogen atoms are represented at the 50% probability level.

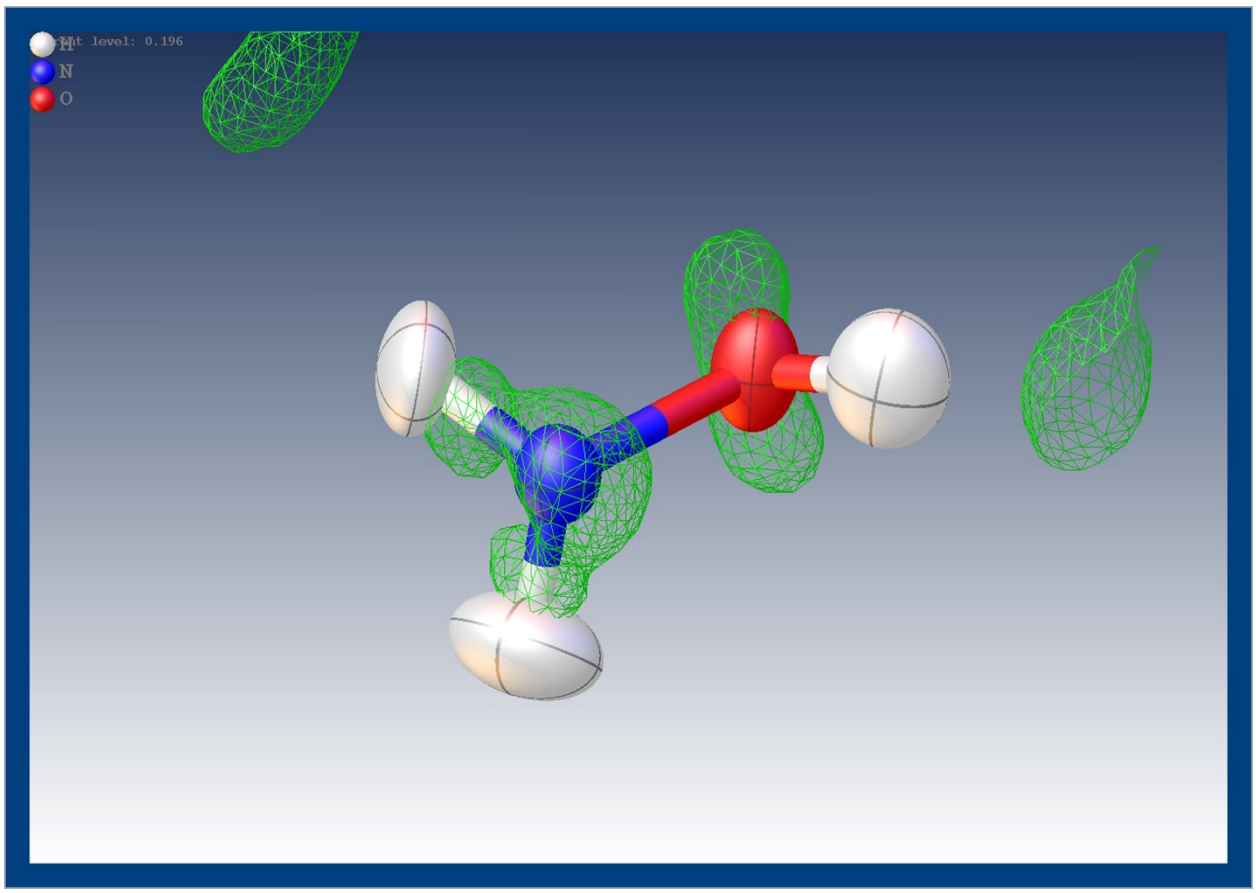

Fig. S10. Deformation electron density map of hydroxylamine (NH_2OH) crystal structure I-100 at 100 K. The green mesh represents positive deformation density, highlighting electron accumulation in chemical bonds and lone pairs (negative deformation density is not observed at this contour level). Calculated with Olex2 using NoSpherA2 (r2SCAN/cc-pVTZ) wave-functions, plotted with an iso-value of 0.196 e/Å³. Anisotropic hydrogen atoms are represented at the 50% probability level.

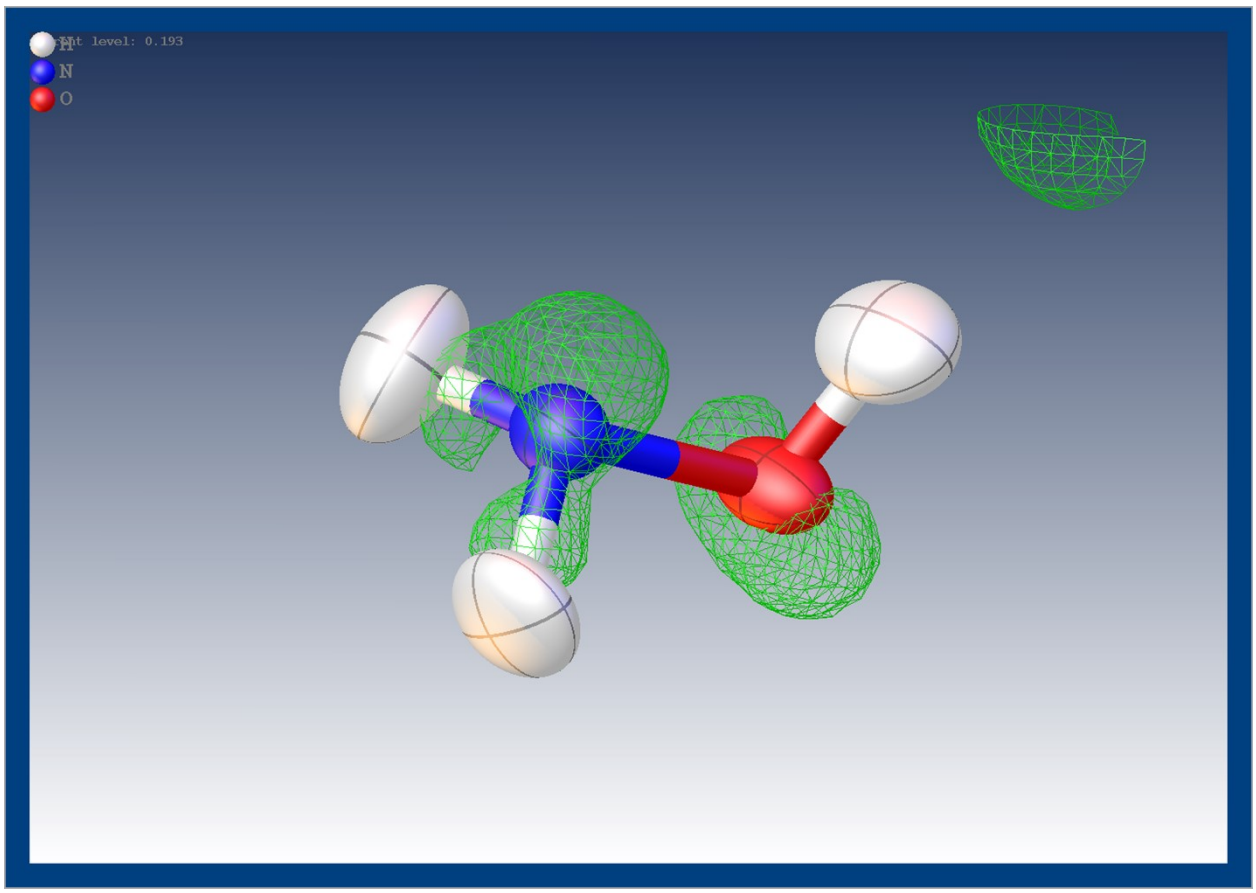

Fig. S11. Deformation electron density map of hydroxylamine (NH_2OH) crystal structure I-100 at 100 K. The green mesh represents positive deformation density, highlighting electron accumulation in chemical bonds and lone pairs (negative deformation density is not observed at this contour level). Calculated with Olex2 using NoSpherA2 (r2SCAN/cc-pVTZ) wave-functions, plotted with an iso-value of 0.193 e/Å³. Anisotropic hydrogen atoms are represented at the 50% probability level.

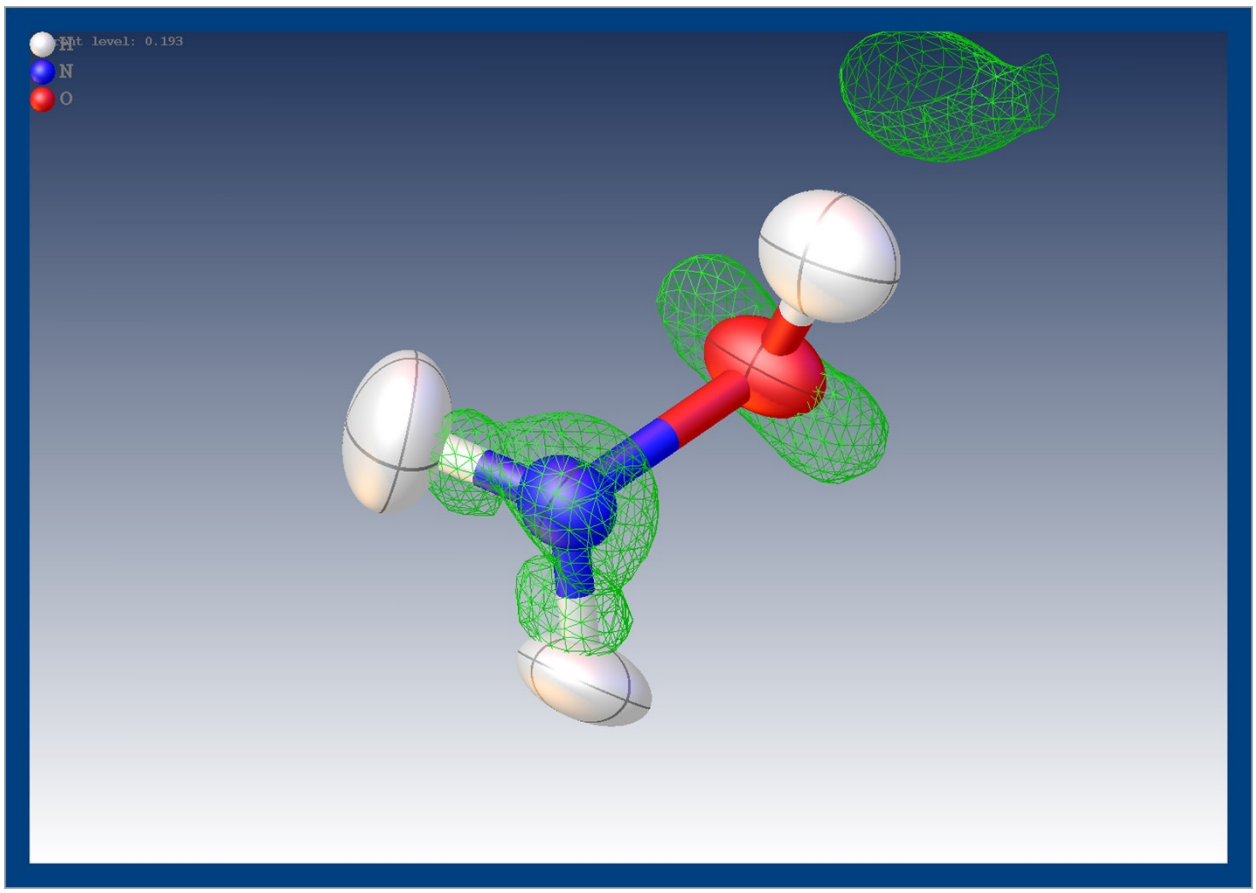

Fig. S12. Deformation electron density map of hydroxylamine (NH_2OH) crystal structure I-100 at 100 K. The green mesh represents positive deformation density, highlighting electron accumulation in chemical bonds and lone pairs (negative deformation density is not observed at this contour level). Calculated with Olex2 using NoSpherA2 (r2SCAN/cc-pVTZ) wave-functions, plotted with an iso-value of 0.193 e/Å^3. Anisotropic hydrogen atoms are represented at the 50% probability level.

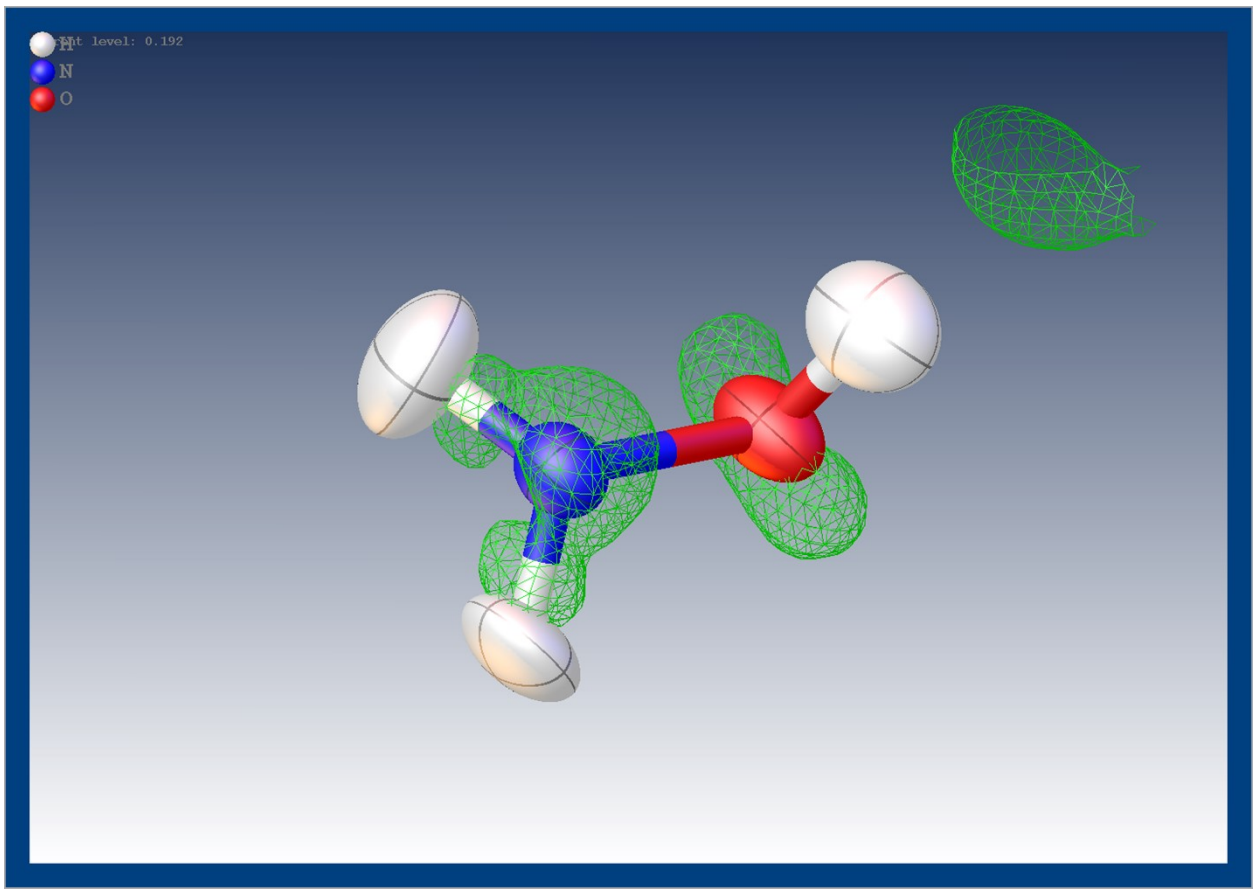

Fig. S13. Deformation electron density map of hydroxylamine (NH_2OH) crystal structure I-100 at 100 K. The green mesh represents positive deformation density, highlighting electron accumulation in chemical bonds and lone pairs (negative deformation density is not observed at this contour level). Calculated with Olex2 using NoSpherA2 (r2SCAN/cc-pVTZ) wave-functions, plotted with an iso-value of 0.192 e/Å^3. Anisotropic hydrogen atoms are represented at the 50% probability level.

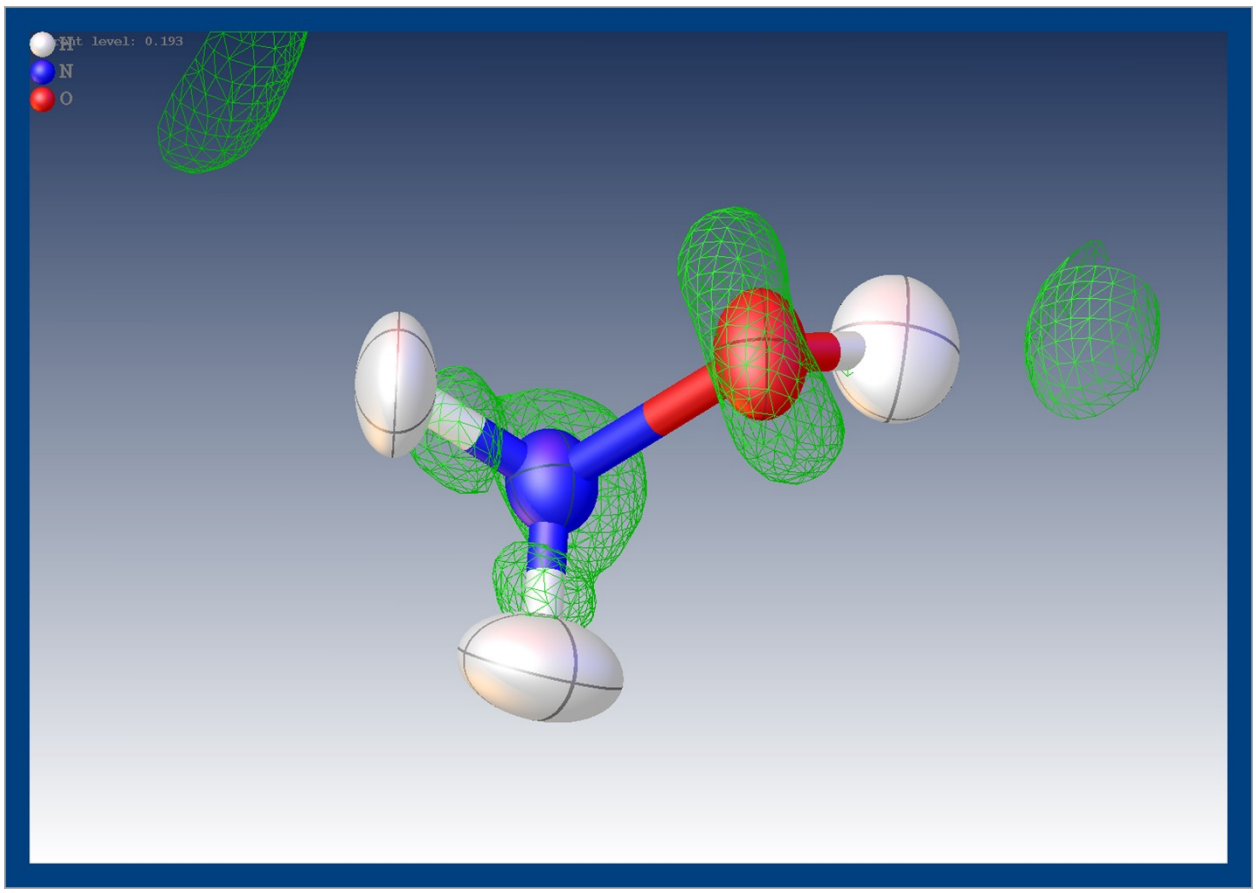

Fig. S14. Deformation electron density map of hydroxylamine (NH_2OH) crystal structure I-100 at 100 K. The green mesh represents positive deformation density, highlighting electron accumulation in chemical bonds and lone pairs (negative deformation density is not observed at this contour level). Calculated with Olex2 using NoSpherA2 (r2SCAN/cc-pVTZ) wave-functions, plotted with an iso-value of 0.193 e/Å^3. Anisotropic hydrogen atoms are represented at the 50% probability level.

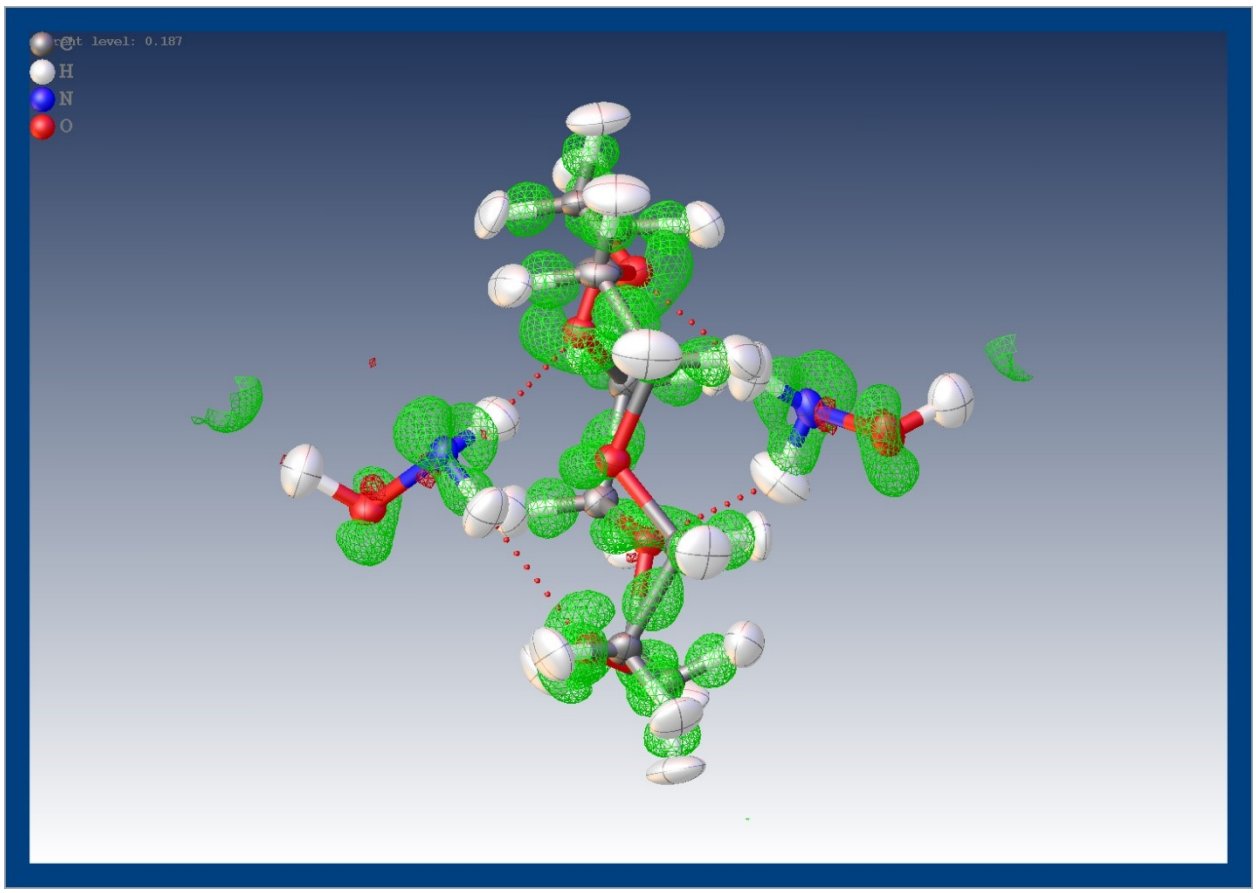

Fig. S15. Deformation electron density map of 15-crown-5 hydroxylaminosolvate ($C_{10}H_{20}O_5 \cdot 2NH_2OH$) crystal structure II at 100 K. The green and red meshes represent positive and negative deformation densities, respectively, highlighting electron accumulation in chemical bonds and lone pairs, calculated with Olex2 using NoSpherA2 (r2SCAN/cc-pVTZ) wave-functions, plotted with an iso-value of 0.187 e/Å^3. Anisotropic hydrogen atoms are represented at the 50% probability level.

Table S1. Crystallographic data and selected parameters of X-ray structural analysis for hydroxylamine structures at various temperatures (**I-100 – I-275**) obtained from spherical (**IAM**) and non-spherical (**NoSpherA2**) refinements.

Structure	**I-100**	**I-150**	**I-200**	**I-250**	**I-265**	**I-270**	**I-275**
Formula	NH_2OH	NH_2OH	NH_2OH	NH_2OH	NH_2OH	NH_2OH	NH_2OH
*F*w	33.03	33.03	33.03	33.03	33.03	33.03	33.03
Crystal system	Orthorhombic	Orthorhombic	Orthorhombic	Orthorhombic	Orthorhombic	Orthorhombic	Orthorhombic
Space group	$P2_12_12_1$	$P2_12_12_1$	$P2_12_12_1$	$P2_12_12_1$	$P2_12_12_1$	$P2_12_12_1$	$P2_12_12_1$
a (Å)	4.4417(3)	4.4508(3)	4.4591(9)	4.4755(4)	4.489(5)	4.481(5)	4.484(5)
b (Å)	4.8184(4)	4.8299(4)	4.8431(11)	4.8703(5)	4.872(7)	4.882(5)	4.884(5)
c (Å)	7.1745(6)	7.1955(6)	7.2097(16)	7.2514(7)	7.233(9)	7.274(8)	7.248(8)
α (deg)	90	90	90	90	90	90	90
β (deg)	90	90	90	90	90	90	90
γ (deg)	90	90	90	90	90	90	90
V (Å^3)	153.55(2)	154.68(2)	155.70(6)	158.06(3)	158.2(3)	159.1(3)	158.7(3)
Z	4	4	4	4	4	4	4
F(000)	72	72	72	72	72	72	72
D_c ($g \cdot cm^{-3}$)	1.429	1.419	1.409	1.388	1.387	1.379	1.382
μ (mm^{-1})	0.141	0.140	0.139	0.137	0.136	0.136	0.136
T, K	100	150	200	250	265	270	275

Refl collcd	2451		2455		2247		2247		2247		2247		2247	
Indep reflns / R_{int}	474 / 0.0442		475 / 0.0456		475 / 0.0507		475 / 0.0507		475 / 0.0507		475 / 0.0507		475 / 0.0507	
Reflns $I>2\sigma(I)$	449		440		420		420		420		420		420	
θ range (deg)	5.097 - 30.528		5.084 - 30.533		5.071 - 30.468		5.043 - 30.302		5.045 - 30.315		5.030 - 30.222		5.034 - 30.286	
No of param	31	46	31	46	31	46	31	46	31	46	31	46	31	46
Refinement	IAM	NoSpherA2	IAM	NoSpherA2	IAM	NoSpherA2	IAM	NoSpherA2	IAM	NoSpherA2	IAM	NoSpherA2	IAM	NoSpherA2
R_1 $[I>2\sigma(I)]$	0.0249	0.0173	0.0250	0.0180	0.0312	0.0238	0.0313	0.0240	0.0310	0.0238	0.0314	0.0241	0.0313	0.0240
wR_2 (all data)	0.0639	0.0401	0.0677	0.0433	0.0858	0.0545	0.0863	0.0549	0.0848	0.0546	0.0866	0.0553	0.0861	0.0549
GooF on F^2	1.154	1.031	1.121	1.005	1.091	0.986	1.096	0.992	1.098	0.987	1.097	0.990	1.097	0.996
Largest diff peak / hole ($e \cdot Å^{-3}$)	0.175 / -0.172	0.103 / -0.087	0.129 / -0.157	0.114 / -0.103	0.167 / -0.197	0.134 / -0.139	0.171 / -0.192	0.135 / -0.136	0.165 / -0.189	0.134 / -0.134	0.172 / -0.191	0.136 / -0.135	0.171 / -0.190	0.135 / -0.135
CCDC number	2557409	2557401	2557410	2557402	2557411	2557403	2557412	2557404	2557413	2557405	2557414	2557406	2557415	2557407

Table S2. Distances and angles describing hydrogen bonds in the structures of neat hydroxylamine at different temperatures (I-100 – I-275) and 15-crown-5 hydroxylaminosolvate (II). Comparison of spherical (**IAM**) and non-spherical (**NoSpherA2**) refinements.

Refinement		N-H…O				O-H…N			
		N-H, Å	H…O, Å	N_H…O, Å	N-H…O, °	O-H, Å	H…N, Å	O_H…N, Å	O-H…N, °
I-100	IAM	0.886(19)	2.46(2)	3.1416(15)	134.1(15)	0.82(2)	1.92(2)	2.7390(12)	178(2)
		0.860(17)	2.244(17)	3.0272(13)	151.4(14)				
	NoSpherA2	1.006(9)	2.377(10)	3.1445(8)	132.5(8)	0.948(11)	1.795(11)	2.7426(7)	179.4(10)
		0.982(11)	2.148(11)	3.0308(8)	148.8(7)				
I-150	IAM	0.876(19)	2.501(19)	3.1569(15)	132.3(15)	0.80(2)	1.94(2)	2.7407(13)	176(2)
		0.876(17)	2.240(17)	3.0384(13)	151.4(14)				
	NoSpherA2	0.997(9)	2.418(11)	3.1605(9)	130.8(8)	0.943(12)	1.802(12)	2.7449(7)	178.7(11)
		0.988(11)	2.151(11)	3.0414(8)	149.1(7)				
I-200	IAM	0.86(2)	2.25(2)	3.0502(17)	153.6(17)	0.78(3)	1.96(3)	2.7426(16)	174(2)
		0.89(2)	2.47(2)	3.1739(19)	136.0(19)				
	NoSpherA2	0.983(13)	2.155(14)	3.0525(12)	151.1(10)	0.925(15)	1.823(15)	2.7476(11)	178.5(14)

		0.998(13)	2.414(15)	3.1768(13)	132.7(11)				
I-250	IAM	0.87(2)	2.27(2)	3.0669(17)	153.6(17)	0.78(3)	1.98(3)	2.7576(16)	174(2)
		0.90(2)	2.48(2)	3.1915(19)	136.0(19)				
	NoSpherA2	0.987(14)	2.167(14)	3.0693(12)	151.2(10)	0.930(15)	1.833(16)	2.7626(10)	178.6(14)
		1.004(13)	2.426(15)	3.1945(13)	132.8(11)				
I-265	IAM	0.89(2)	2.49(2)	3.188(3)	135.8(19)	0.79(3)	1.98(3)	2.758(3)	174(2)
		0.87(2)	2.27(2)	3.067(4)	153.6(17)				
	NoSpherA2	0.987(13)	2.168(14)	3.069(3)	151.1(10)	0.929(15)	1.834(16)	2.763(3)	178.5(14)
		1.002(14)	2.430(15)	3.198(3)	132.8(11)				
I-270	IAM	0.87(2)	2.27(2)	3.074(3)	153.6(17)	0.79(3)	1.98(3)	2.764(2)	174(2)
		0.90(2)	2.49(2)	3.200(3)	136.1(19)				
	NoSpherA2	0.989(14)	2.173(14)	3.077(2)	151.2(10)	0.932(15)	1.837(16)	2.769(2)	178.6(14)
		1.007(14)	2.432(15)	3.203(3)	132.8(11)				
I-275	IAM	0.90(2)	2.49(2)	3.195(3)	136.0(19)	0.79(3)	1.98(3)	2.763(3)	174(2)

		0.87(2)	2.27(2)	3.073(3)	153.6(17)				
	NoSpherA2	0.989(13)	2.172(14)	3.076(3)	151.2(10)	0.930(15)	1.838(16)	2.768(2)	178.5(14)
		1.004(14)	2.430(15)	3.198(3)	132.8(11)				
II	IAM	0.899(14)	2.115(14)	2.9929(11)	165.3(12)	0.846(15)	1.949(15)	2.7595(10)	160.0(13)
		0.902(14)	2.177(14)	2.9267(10)	140.1(11)				
	NoSpherA2	1.014(9)	2.004(9)	2.9978(7)	166.0(7)	0.974(9)	1.830(9)	2.7584(7)	158.2(7)
		1.006(8)	2.084(9)	2.9321(7)	140.6(7)				
	IAM	0.910(12)	2.259(12)	3.1367(10)	161.8(10)	0.872(15)	1.938(15)	2.7734(10)	159.9(13)
		0.893(12)	2.112(13)	2.9977(10)	171.0(11)				
	NoSpherA2	1.020(7)	2.158(8)	3.1376(7)	160.5(6)	0.975(9)	1.842(9)	2.7736(7)	158.7(8)
		1.007(8)	2.004(8)	3.0006(7)	170.0(7)				

Table S3. Crystallographic data and selected parameters of X-ray structural analysis for the molecular structure of the 15-crown-5 hydroxylaminosolvate (II) obtained from spherical (**IAM**) and non-spherical (**NoSpherA2**) refinements.

Structure	**II**	
Formula	$C_{10}H_{20}O_5 \cdot 2NH_2OH$	
*F*w	286.33	
Crystal system	Moniclinic	
Space group	$P2_1/c$	
a (Å)	11.7376(4)	
b (Å)	10.1973(3)	
c (Å)	12.6543(4)	
α (deg)	90	
β (deg)	104.2070(10)	
γ (deg)	90	
V (Å^3)	1468.29(8)	
Z	4	
F(000)	624	
D_c *(g·cm^{-3})*	1.295	
μ (mm^{-1})	0.108	
T, K	**100**	
Refl collcd	23843	
Indep reflns / R_{int}	4485 / 0.0408	
Reflns $I>2\sigma(I)$	3712	
θ range (deg)	1.790 – 30.55	
No of param	276	406
Rifenement	IAM	NoSpherA2
R_1 $[I>2\sigma(I)]$	0.0356	0.0250
wR_2 (all data)	0.0947	0.0520
GooF on F^2	1.025	1.054
Largest diff peak / hole (e·Å^{-3})	0.304 / –0.215	0.185 / –0.199

CCDC number	2557416	2557408

Table S4. Intramolecular bond lengths (Å) and angles (°) in hydroxylamine: literature data from 1955 (*), neat hydroxylamine at various temperatures (I-100 – I-275), and the 15-crown-5 hydroxylaminosolvate (II). Comparison of spherical (**IAM**) and non-spherical (**NoSpherA2**) refinements.

	Refinement	N-O, Å	O-H, Å	N-H, Å	N-O-H, °	O-N-H, °	H-N-H, °	H-O-N-H, °
*NH_2OH**		*1.47(3)*	—				—	
I-275	IAM	1.446(2)	0.79(3)	0.90(2); 0.87(2)	105.2(17)	108.2(15); 102.2(13)	111(2)	101(2); -142(2)
	NoSpherA2	1.4375(17)	0.930(15)	1.004(14); 0.989(13)	102.4(8)	107.4(9); 102.0(7)	108.4(11)	—
I-270	IAM	1.445(2)	0.79(3)	0.87(2); 0.90(2)	105.3(18)	102.1(13); 108.2(15)	111(2)	-142(2); 101(2)
	NoSpherA2	1.4371(17)	0.932(15)	0.989(14); 1.007(14)	102.4(8)	102.0(7); 107.4(9)	108.4(11)	—
I-265	IAM	1.447(2)	0.79(3)	0.89(2); 0.87(2)	105.3(17)	108.1(15); 102.3(13)	111(2)	101(2); -142(2)
	NoSpherA2	1.4384(18)	0.929(15)	1.002(14); 0.987(13)	102.5(8)	107.3(9); 102.2(7)	108.3(11)	—
I-250	IAM	1.4431(18)	0.78(3)	0.87(2); 0.90(2)	105.4(17)	102.2(13); 108.2(15)	111(2)	-142(2); 101(2)

	NoSpherA2	1.4350(11)	0.930(15)	0.987(14); 1.004(13)	102.4(8)	102.0(7); 107.4(9)	108.4(11)	—
I-200	IAM	1.4374(18)	0.78(3)	0.86(2); 0.89(2)	105.4(17)	102.3(13); 108.2(15)	111(2)	142(2); -101(2)
	NoSpherA2	1.4293(11)	0.925(15)	0.983(13); 0.998(13)	102.4(8)	102.1(7); 107.3(9)	108.3(11)	—
I-150	IAM	1.4453(16)	0.80(2)	0.876(19); 0.875(19)	103.9(14)	107.7(13); 102.9(11)	108.2(17)	105.8(16); -140.0(15)
	NoSpherA2	1.4351(8)	0.943(12)	0.997(9); 0.988(11)	103.0(7)	107.1(7); 103.4(6)	106.4(8)	—
I-100	IAM	1.4491(15)	0.82(2)	0.886(19); 0.868(19)	103.4(14)	106.8(13); 102.7(11)	109.3(17)	105.5(19); -139.8(19)
	NoSpherA2	1.4391(7)	0.948(11)	1.006(9); 0.982(11)	102.2(6)	106.5(6); 103.1(5)	107.8(8)	—
N1-O1 in **II**	IAM	1.4497(10)	0.846(15)	0.899(14); 0.902(14)	99.4(9)	103.1(9); 102.6(8)	105.0(12)	-125.0(13); 126.1(13)
	NoSpherA2	1.4413(7)	0.974(9)	1.014(9); 1.006(8)	100.0(5)	105.1(5); 105.3(5)	105.6(7)	—

N2-O2 in **II**	IAM	1.4569(10)	0.872(15)	0.910(12); 0.893(12)	100.3(9)	104.0(7); 103.2(8)	105.5(10)	131.9(12); -118.1(12)
	NoSpherA2	1.4489(7)	0.975(9)	1.020(7); 1.007(8)	100.8(5)	105.5(5); 104.8(4)	104.4(6)	—
Ranges	IAM	1.4374(18) – 1.4569(10)	0.78(3) – 0.872(15)	0.86(2) – 0.910(12)	99.4(9) – 105.4(17)	102.1(13) – 108.2(15)	105.0(12) – 111(2)	от -142(2) до 142(2)
	NoSpherA2	1.4293(11) – 1.4489(7)	0.925(15) – 0.975(9)	0.982(11) – 1.020(7)	100.0(5) – 103.0(7)	102.0(7) – 107.4(9)	104.4(6) – 108.4(11)	—

* E. A. Meyers and W. N. Lipscomb, *Acta Cryst*, 1955, **8**, 583–587.

Table S5. Crystalline structures containing hydroxylamine in zwitterionic ($NH_3^+O^-$) or neutral (NH_2OH) form.

№	refcode	$NH_3^+O^-$ or NH_2OH	d(N-O), Å	Notes
1	LUDCES	NH_2OH	1.446, 1.448	H not located
2	LUDCOC	NH_2OH	1.447	H not located
3	YEKJEF	$NH_3^+O^-$	1.4198	H from difference map
4	CUPZAQ	$NH_3^+O^-$	1.409	H from difference map
5	RARCEV	$NH_3^+O^-$	1.4127	H from difference map
6	GIMNOI	$NH_3^+O^-$	1.4181	H from difference map
7	UFUBAB	$NH_3^+O^-$	1.414	H from difference map
8	UFUBEF	$NH_3^+O^-$	1.399, 1.411	Mix
9	SUCDEC	NH_2OH	1.313	Disordered
10	AXOZAR	$NH_3^+O^-$	1.3996	H calculated
11	IDAWOD	$NH_3^+O^-$	1.409	H calculated
12	ILEQOI	$NH_3^+O^-$	1.4164	H calculated
13	LAWGOJ	NH_2OH	1.480	Disordered
14	KIXNEO	$NH_3^+O^-$	1.406	H calculated
15	LERJUR	$NH_3^+O^-$	1.4087	H from difference map
16	REYSIB	$NH_3^+O^-$	1.4208, 1.4218	H calculated
17	BISTAC	$NH_3^+O^-$ and NH_2OH	1.407 and 1.412	H calculated
18	UFOQUF	$NH_3^+O^-$	1.417	H from difference map
19	NOLROZ	NH_2OH	1.350	Disordered

20	DUKVAK	NH_2OH	1.546	Disordered
21	BAGHAX	$NH_3^+O^-$	1.419	H from difference map
22	BAGHAB	$NH_3^+O^-$	1.415	H from difference map
23	ULENUY	NH_2OH	1.401, 1.405, 1.411, 1.430	H calculated
24	ULEPEK	$NH_3^+O^-$	1.401	H calculated
II	2557416, IAM	NH_2OH	1.4497(10), 1.4569(10)	H from difference map
	2557408, NoSpherA2	NH_2OH	1.4413(7), 1.4489(7)	
I-100	2557409, IAM	NH_2OH	1.4491(15)	H from difference map
	2557401, NoSpherA2	NH_2OH	1.4391(7)	
*		NH_2OH	1.47(3)	H not located

* E. A. Meyers and W. N. Lipscomb, *Acta Cryst*, 1955, **8**, 583–587.

Details of periodic (solid-state) DFT calculations.

In the CRYSTAL17 calculations [s1], we employed the PBE [s2] and B3LYP [s3,s4] functionals with the 6-31G** basis set. The sequential introduction of dispersion corrections in the B3LYP method is not unambiguous [s5-s7]. Therefore, London dispersion interactions were taken into account by introducing the D3 correction with Becke-Jones damping [s8], as implemented in CRYSTAL17, only in PBE calculations.

The CRYSTAL parameters describing the level of accuracy in evaluating the Coulomb and Hartree–Fock exchange series were set to 7 7 7 7 15. Tolerances on energies which control the self-consistent field convergence for geometry optimizations and frequency computations were set to 1×10^{-10} and 1×10^{-11} Hartree, respectively. The shrinking factor of the reciprocal space net was set to 3. The space group and the unit cell parameter of the considered crystal obtained from the X-ray diffraction experiment were fixed, and the structural relaxations were restricted to the positional parameters of the atoms (AtomOnly parameter in Crystal17). The analysis of normal vibrations does not reveal imaginary frequencies for crystals under consideration.
It was assumed that intermolecular hydrogen bond is realized when there is a point (3,-1) on the bond path [s9] between two atoms belonging to different molecules. Bader analysis of the crystalline electron density is carried out using Topond14 [s10].

In the present study, the ΔHHB values were evaluated using the Rozenberg equation [s11]:

$$-\Delta H_{HB}\ [\text{kJ mol}^{-1}] = 0.134 \cdot R(\text{H}\cdots\text{O})^{-3.05}, \qquad \text{(s1)}$$

Where the R(H···O) is the H···O distance (nm). The empirical correlation (s1) gives the ΔH_{HB} values of intermolecular H-bonds in molecular crystals in the range of 10 − 80 kJ/mol with the accuracy around several kJ/mol [s11].

References.

s1. Dovesi, R.; Erba, A.; Orlando, R.; Zicovich-Wilson, C.M.; Civalleri, B.; Maschio, L.; Rérat, M.; Casassa, S.; Baima, J.; Salustro, S.; Kirtman, B. Quantum-Mechanical Condensed Matter Simulations with CRYSTAL. WIREs Comput. Mol. Sci. 2018, 8, e1360. https://doi.org/10.1002/wcms.1360

s2. Perdew, J.P.; Burke, K.; Ernzerhof, M. Generalized Gradient Approximation Made Simple. Phys. Rev. Lett. 1996, 77, 3865–3868. https://doi.org/10.1103/PhysRevLett.77.3865

s3. Becke, A.D. Density-Functional Thermochemistry. III. The Role of Exact Exchange. J. Chem. Phys. 1993, 98, 5648–5652. https://doi.org/10.1063/1.464913

s4. Lee, C.; Yang, W.; Parr, R.G. Development of the Colle-Salvetti Correlation-Energy Formula into a Functional of the Electron Density. Phys. Rev. B 1988, 37, 785–789. https://doi.org/10.1103/PhysRevB.37.785

s5. Goerigk, L.; Grimme, S. A Thorough Benchmark of Density Functional Methods for General Main Group Thermochemistry, Kinetics, and Noncovalent Interactions. Phys. Chem. Chem. Phys. 2011, 13, 6670. https://doi.org/10.1039/c0cp02984j

s6. Katsyuba, S.A.; Vener, M.V.; Zvereva, E.E.; Brandenburg, J.G. The Role of London Dispersion Interactions in Strong and Moderate Intermolecular Hydrogen Bonds in the Crystal and in the Gas Phase. Chem. Phys. Lett. 2017, 672, 124–127. https://doi.org/10.1016/j.cplett.2017.01.070

s7. Merten, C. Modelling Solute–Solvent Interactions in VCD Spectra Analysis with the Micro-Solvation Approach. Phys. Chem. Chem. Phys. 2023, 25, 29404–29414. https://doi.org/10.1039/D3CP03408A

s8. Grimme, S.; Ehrlich, S.; Goerigk, L. Effect of the Damping Function in Dispersion Corrected Density Functional Theory. J. Comput. Chem. 2011, 32, 1456–1465. https://doi.org/10.1002/jcc.21759

s9. Bader, R.F.W. A Quantum Theory of Molecular Structure and Its Applications. Chem. Rev. 1991, 91, 893–928. https://doi.org/10.1021/cr00005a013

s10. Gatti, C.; Casassa, S. TOPOND-2013: an electron density topological program for systems periodic in N (N=0-3) dimensions, User's Manual - CNR-CSRSRC, Milano, Italy, 2013.

s11. Rozenberg, M.; Loewenschuss, A.; Marcus, Y. An Empirical Correlation Between Stretching Vibration Redshift and Hydrogen Bond Length. *Phys. Chem. Chem. Phys.* **2000**, *2*, 2699–2702

Table S6. Distance between "heavy" atoms d(O···N)/d(N···O) of hydrogen bonds in the studied crystals. Experiment vs. periodic DFT computations in the and B3LYP/6-31G** and PBE-D3/6-31G** levels. Units are Å.

c	X-ray	B3LYP	PBE-D3
Crystal I			
O(1)–H(1)···N(1A)	2.739	2.696	2.625
N(1)–H(2)···O(1B)	3.142	3.177	3.166
N(1)–H(3)···O(1C)	3.027	2.932	2.889
Crystal II			
O(1)–H(1)···N(1A)	2.760.	2.736	2.705
N(1)–H(11)···O(5)	2.993	2.969	2.956
N(1)–H(12)···O(3)	2.927	2.952	2.948
O(2)–H(2)···N(2A)	2.773	2.746	2.713
N(2)–H(21)···O(7)	3.137	3.086	3.086
N(2)–H(22)···O(4)	2.998	2.985	2.974

Table S7. The electron density ρ_b and its Laplacian $\nabla^2\rho_b$ at the (3,-1) critical point of intermolecular hydrogen bonds in crystals I and II calculated using periodic DFT computations in the and B3LYP/6-31G** and PBE-D3/6-31G** levels.

Fragment	B3LYP		PBE-D3	
	ρ_b, a.u.	$\nabla^2\rho_b$, a.u.	ρ_b, a.u.	$\nabla^2\rho_b$, a.u.
Crystal I				
O(1)–H(1)···N(1A)	0.0586	0.1112	0.0784	0.0940
N(1)–H(2)···O(1B)	0.0260	0.0721	0.0301	0.0801
N(1)–H(3)···O(1C)	0.0122	0.0378	0.0190	0.0466
Crystal II				
O(1)–H(1)···N(1A)	0.0461	0.1020	0.0536	0.1032
N(1)–H(11)···O(5)	0.0251	0.0723	0.0260	0.0718
N(1)–H(12)···O(3)	0.0256	0.0738	0.0276	0.0768
O(2)–H(2)···N(2A)	0.0452	0.1007	0.0527	0.1022
N(2)–H(21)···O(7)	0.0197	0.0538	0.0212	0.0550
N(2)–H(22)···O(4)	0.0249	0.0722	0.0267	0.0740

Selection criteria for statistical analysis

The proposed geometric criterion for distinguishing between molecular NH_2OH and zwitterionic $NH_3^+O^-$ is based exclusively on Independent Atom Model (IAM) refinement data. This choice is justified by two considerations: (i) the vast majority of structures deposited in the Cambridge Structural Database (CSD) are refined using the IAM, and (ii) IAM remains the standard approach in routine X-ray diffraction analysis. Therefore, to ensure broad applicability of the criterion, it must be derived from IAM data.

Furthermore, only structures meeting the following strict quality criteria were included in the analysis:

Unequivocal assignment of the hydroxylamine form — the structure must be unambiguously reported as either NH_2OH or $NH_3^+O^-$ based on the original authors' interpretation.

Hydrogen atoms located from Fourier difference maps — no geometrically placed or calculated hydrogen atoms were allowed, as this may bias the N–O bond length.

Absence of disorder — disorder involving the N or O atoms of hydroxylamine can artificially shorten or lengthen the observed N–O distance and therefore such structures were excluded.

For the NH_2OH and $NH_3^+O^-$ datasets, all nine structures in each set satisfy these strict criteria.

For the NH_3OH^+ cation, the CSD initially returned approximately 300 fragments. Rather than manually inspecting all entries, we focused the validation on the extreme lower and upper tails of the N–O bond length distribution — i.e., the regions where the choice of refinement model or data quality could most significantly affect the 3σ boundaries. Structures in these boundary regions that exhibited disorder, unrealistic N–O distances, geometric placement of hydrogen atoms, or obvious refinement errors were discarded. After this targeted screening, 256 structures remained for statistical analysis. We note that the vast majority of structures in the central part of the distribution have N–O bond lengths well within the expected range for NH_3OH^+, and their inclusion does not affect the calculated 3σ limits

The resulting statistical parameters are summarized in Table S8. Critically, the N–O bond length alone cannot distinguish between $NH_3^+O^-$ and NH_3OH^+ due to the significant overlap of their 3σ intervals (1.4271 vs. 1.4353 Å). Differentiation between these two species requires analysis of the ionic environment (e.g., the presence of counterions).

Table S8. Statistical parameters of N–O bond lengths for NH_2OH, $NH_3^+O^-$ and NH_3OH^+.

Species	n	μ (Å)	σ (Å)	μ – 3σ (Å)	μ + 3σ (Å)	Criterion
NH_2OH	9	1.4466	0.0053	1.4308	1.4625	d(N–O) > 1.43 Å
$NH_3^+O^-$	9	1.4148	0.0041	1.4025	1.4271	d(N–O) ≤ 1.43 Å*
NH_3OH^+	256	1.4095	0.0086	1.3838	1.4353	d(N–O) ≤ 1.43 Å*

**For d(N–O) ≤ 1.43 Å, distinction between $NH_3^+O^-$ and NH_3OH^+ requires analysis of the ionic environment.*

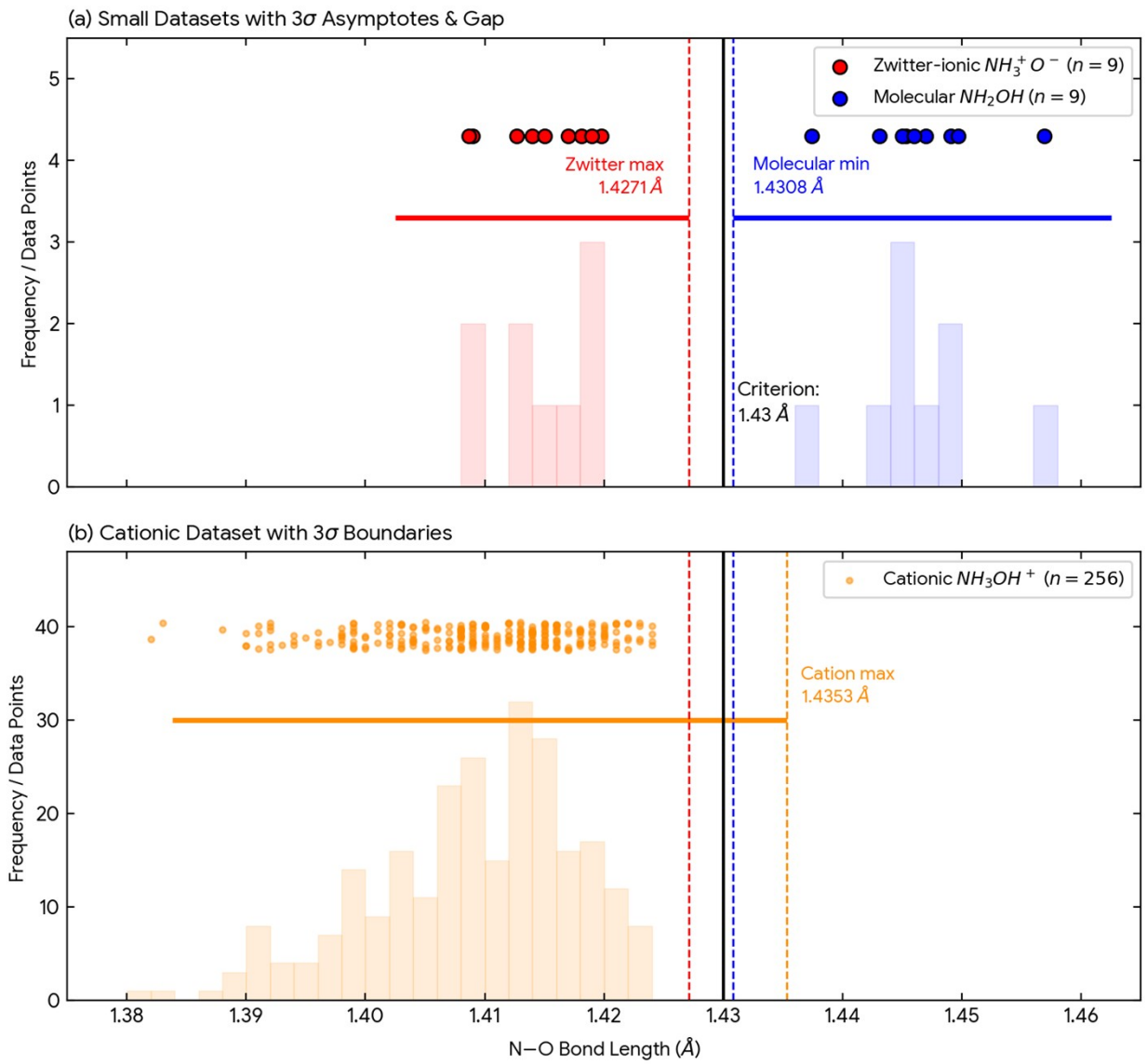

Fig. S16. Statistical analysis of N–O bond lengths for molecular NH_2OH (blue, n=9, this work), zwitterionic $NH_3^+O^-$ (red, n=9, CSD), and cationic NH_3OH^+ (orange, n=256, CSD). The solid vertical black line at 1.43 Å defines the diagnostic threshold. Coloured dashed lines indicate the 3σ boundaries. The gap between the blue and red 3σ intervals (1.4308 vs. 1.4271 Å) validates the criterion for distinguishing NH_2OH from $NH_3^+O^-$, while the overlap with the orange interval (up to 1.4353 Å) shows that N–O bond length alone cannot differentiate $NH_3^+O^-$ from NH_3OH^+.